A biodegradable and biocompatible gecko-inspired tissue adhesive

Alborz Mahdavi*, Lino Ferreira*†, Cathryn Sundback‡§, Jason W. Nichol¶, Edwin P. Chan¶, David J. D. Carter∥, Chris J. Bettinger¶, Siamrut Patanavanich*, Loice Chignozha*, Eli Ben-Joseph*, Alex Galakatos*, Howard Pryor‡§, Irina Pomerantseva‡§, Peter T. Masiakos§**, William Faquin§††, Andreas Zumbuehl‡‡, Seungpyo Hong*, Jeffrey Borenstein∥, Joseph Vacanti‡§**, Robert Langer*¶§§, and Jeffrey M. Karp§¶§§¶¶

*Department of Chemical Engineering, Massachusetts Institute of Technology, Cambridge, MA 02139-4307; †Center of Neurosciences and Cell Biology, University of Coimbra, and Biocant Biotechnology Innovation Center, 3060-197 Cantanhede, Portugal; ‡Center for Regenerative Medicine and Departments of **Pediatric Surgery and ††Pathology, Massachusetts General Hospital, Boston, MA 02114; §Harvard Medical School, Boston, MA 02115; ¶Harvard–Massachusetts Institute of Technology, Division of Health Science and Technology, Cambridge, MA 02139; ∥The Charles Stark Draper Laboratory, Cambridge, MA 02139-3563; ‡‡Biozentrum, University of Basel, Klingelbergstrasse 50/70, 4056 Basel, Switzerland; and ¶¶Health Sciences and Technology, Center for Biomedical Engineering, Brigham and Women's Hospital, Boston, MA 02115

There is a significant medical need for tough biodegradable polymer adhesives that can adapt to or recover from various mechanical deformations while remaining strongly attached to the underlying tissue. We approached this problem by using a polymer poly(glycerol-co-sebacate acrylate) and modifying the surface to mimic the nanotopography of gecko feet, which allows attachment to vertical surfaces. Translation of existing gecko-inspired adhesives for medical applications is complex, as multiple parameters must be optimized, including: biocompatibility, biodegradation, strong adhesive tissue bonding, as well as compliance and conformability to tissue surfaces. Ideally these adhesives would also have the ability to deliver drugs or growth factors to promote healing. As a first demonstration, we have created a gecko-inspired tissue adhesive from a biocompatible and biodegradable elastomer combined with a thin tissue-reactive biocompatible surface coating. Tissue adhesion was optimized by varying dimensions of the nanoscale pillars, including the ratio of tip diameter to pitch and the ratio of tip diameter to base diameter. Coating these nanomolded pillars of biodegradable elastomers with a thin layer of oxidized dextran significantly increased the interfacial adhesion strength on porcine intestine tissue *in vitro* and in the rat abdominal subfascial *in vivo* environment. This gecko-inspired medical adhesive may have potential applications for sealing wounds and for replacement or augmentation of sutures or staples.

chemical cross-link | medical adhesive | nanotopography | surgical suture

The ability of gecko feet to adhere to vertical and inverted surfaces (1–7) has prompted this study to assess the impact of gecko-like morphology on the properties of chemical reaction based tissue adhesives. Fibrillar arrays, which cover the bottom of gecko feet, maximize the interfacial adhesion to surfaces. Specifically, the adhesive footpads are decorated with a dense array of fibrils (setae); each seta has numerous terminal projections (spatulae) that are 200–500 nm in length (1, 2). The combination of van der Waals (3) and capillary forces (5) controls the adhesion of these spatulae to surfaces. Based on this understanding, synthetic gecko adhesives (8, 9) have been developed that recapitulate these two gecko adhesion features: (*i*) adhesion in a dry environment without a chemical "glue" and (*ii*) a fibrillar design that enhances interface compliance and conformability to surfaces with a variety of roughness.

Despite the growing interest in developing gecko-inspired medical adhesives, only a single adhesive has been optimized for a wet tissue-like environment. Specifically, important work from P. Messersmith's group has demonstrated a synthetic gecko adhesive that is effective under water with reversible noncovalent bonding to inorganic surfaces (10). However, adhesives for medical applications require strong irreversible bonds to organic substrates to avoid

disruption by the movement of underlying or nearby tissues. Furthermore, the bond strengths of experimental adhesives must be tested under physiological conditions. To our knowledge, *in vivo* studies have not been reported with gecko-inspired surfaces. The bond strengths of gecko-inspired adhesives are typically evaluated through submicrometer atomic force microscopy measurements, which may not be predictive of macroscopic patch performance.

In this study, a gecko-inspired tissue adhesive was developed that is elastomeric, biocompatible, and biodegradable. This adhesive is based on poly(glycerol sebacate acrylate) (PGSA), a tough biodegradable elastomer (11, 12) with elastic and biodegradation properties that can be tuned for specific tissue applications and can be easily doped with growth factors or drugs (11). Through combined morphology and chemistry effects, we have demonstrated a biocompatible tissue adhesive with promising covalent cross-linking to wet tissue. This tape-based tissue adhesive platform may have application in medical therapies ranging from suture/staple replacements/supplements; waterproof sealants for hollow organ anatomoses; mesh grafts to treat hernias, ulcers, and burns; and hemostatic wound dressings.

Results and Discussion

Development of Biodegradable Elastomeric Gecko-Inspired Nanopatterns. A fabrication procedure for manufacturing tissue adhesives was developed that avoids high-temperature and harsh chemical conditions that is amenable to a variety of materials. Silicon templates were prepared by using the microfabrication techniques of photolithography and reactive ion etching. To create the nanopattern (Fig. 1a), linear PGSA polymer was cast on nanomold cavities, without high vacuum, and cured by UV light in <5 min at room temperature. To determine the impact of pattern dimensions on PGSA adhesive properties, pillar arrays were patterned in PGSA with tip pillar diameters ranging from ≈100 nm to 1 μm and pillar heights from ≈0.8 to ≈3 μm (Fig. 1b).

The adhesive strength of gecko surfaces to wet substrates depends on the hydrophobic and hydrophilic nature of the substrates and is significantly lower than on dry substrates (3, 6). A recent innovative study for gecko adhesives that work under wet conditions
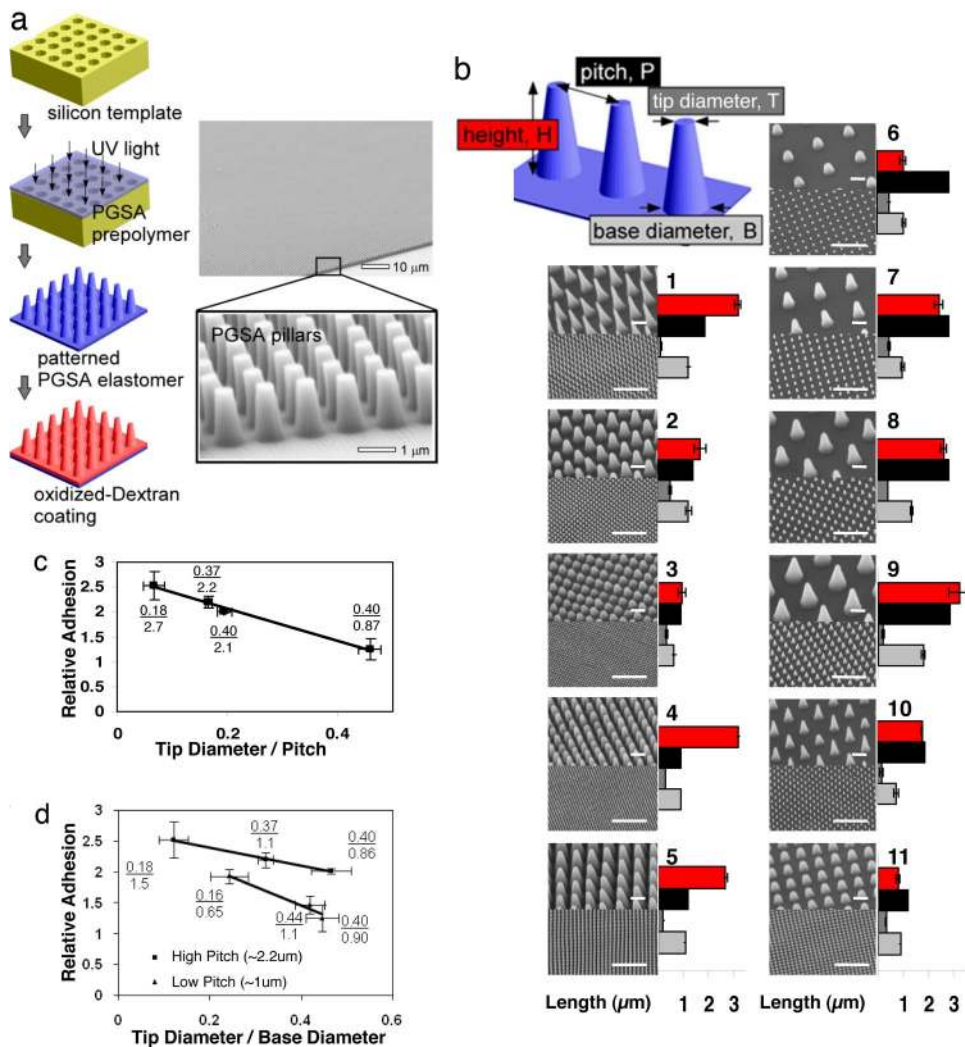
APPLIED BIOLOGICAL SCIENCES

Fig. 1. Development of biodegradable synthetic gecko patterns. (*a*) Nanomolding of the PGSA prepolymer is accomplished by photocuring the prepolymer under UV light followed by removal of the pattern and subsequent spin coating of DXTA on the surface of the pillars. SEM demonstrated excellent pattern transfer and fidelity. (*b*) Gecko patterns having different pillar size and center to center pitch were developed as illustrated by the SEM images. Pillar dimensions were measured by using optical profilometry as represented by the bar graphs, with red representing the height of pillars; black, the center to center pitch; light gray, diameter of pillar base; and dark gray, diameter of the tip. (Small and large scale bars, 1 and 10 μm, respectively.) (*c*) Adhesion trend of the longest pillar heights (2.4 μm) shows adhesion of nanopattern with respect to flat polymer as a function of ratio of tip diameter to pitch. R^2 value of linear fit is 0.99. (*d*) Adhesion trend of the patterns is plotted as a function of ratio of tip diameter to base diameter of pillars. R^2 values of linear fit for the low- and high-pitch patterns are 0.96 and 0.99, respectively.

tested adhesion based on a variety of single pillar measurements to demonstrate the relationship between adhesion strength and pillar geometry (10). However, it is difficult to use these data to accurately predict adhesion strengths of pillar array patterns because of the interactions among individual pillars (10). Furthermore, gecko-inspired adhesives have not been tested on biological tissues. To model physiological tissue conditions, we conducted *in vitro* tests to determine the adhesion strength of PGSA nanopatterned substrates to porcine intestinal tissue. Shear or sliding forces were used to mimic the potential shear forces experienced by tissue adhesives after surgical placement (13). From the force vs. displacement result of the shear adhesion test [supporting information (SI) Fig. 5], we use the maximum separation force as a descriptor of adhesion for all materials. The adhesion strength of nanopatterned PGSA was nearly 2-fold greater than the adhesion strength of flat unpatterned polymer (Fig. 1 *c* and *d*).

To screen the dependence of tissue adhesion on the interfacial contact geometry, we tested tissue adhesion strength as a function of tip diameter to pitch length for the patterns with the longest pillars (2.4 μm). As demonstrated in Fig. 1*c*, a decrease in the ratio of tip diameter to pitch leads to a decrease in tissue adhesion. To demonstrate the importance of pillar geometry on adhesion independently of pillar height, we measured tissue adhesion as a function of ratio of tip diameter to base diameter. As demonstrated in Fig. 1*d*, an increase in this ratio leads to a decrease in adhesion and moreover, this observation holds at different pitch lengths. A

decrease in pitch leads to a decrease in overall adhesion and a sharper fall in adhesion strength with increasing ratio of tip diameter to base diameter of the pillars as demonstrated in Fig. 1*d*. Of the patterns tested, pattern 9 from Fig. 1*b* provided the highest tissue adhesion and therefore was selected for further development of tissue adhesive tape.

Surface Modification of Gecko Patterns for Tissue Interfacing. For the purposes of tissue adhesion, the adhesive must work under water and remain well adhered to the tissue over the course of the healing process. Aldehyde-functionalized polysaccharides have been effectively used in animal models to bond hydrogel materials to tissue proteins with minimal host inflammation (14). Therefore, we coated our gecko-based PGSA adhesives with a thin layer of oxidized dextran (DXT), which has aldehyde functionalities [DXT aldehyde (DXTA)] to promote covalent cross-linking with tissue (Fig. 2*a*). The terminal aldehyde group in DXTA reacts with resident amine groups in proteins forming an imine (15). Furthermore, the aldehyde groups of DXTA can form a hemiacetal with free hydroxyl groups from the glycerol subunit of our PGSA polymer surface.

DXTA with a degree of oxidation of 14% (as confirmed by ^{1}H-NMR) was coated on the surface of gecko nanopatterns by spin coating (Fig. 1*A*). The DXTA-coated nanopatterns were then rinsed extensively with deionized water and characterized by FTIR spectroscopy (Fig. 2*b*). The peak at 3,300 cm^{-1} corresponding to the
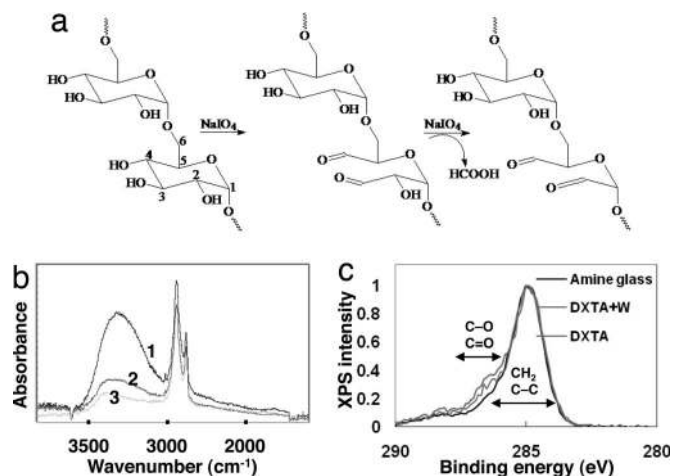
Fig. 2. DXTA coating of gecko surfaces. (*a*) Oxidation of DXT by sodium periodate yielding DXT functionalized with aldehyde groups. (*b*) FTIR spectra of PGSA network coated with DXTA (1, 2) or DXT (3), before (1) or after being washed with water (2, 3). The higher absorbance at 3,300 cm^{-1} (normalized by the absorbance at 2,930 cm^{-1} corresponding to the stretching of C–H bonds) in PGSA nanopatterns coated with DXTA rather than with DXT is indirect evidence that DXTA remained on the surface of the PGSA to a higher extent than DXT, after washing. (*c*) C1s XPS high-resolution spectra of amine-functionalized glass and amine-functionalized glass coated with DXTA before and after being washed with water. The shift in spectra at positions 286–288 eV corresponding to the carbon–oxygen bond shows the presence of DXTA on the surface after rinsing with water (DXTA +W). Data were normalized to the C–C and C-H spectra peak at 285 eV.

stretching of the O–H groups in the glucose units of DXT was used to verify the immobilization of DXTA in the PGSA nanopattern. The higher absorbance at 3,300 cm^{-1} in PGSA nanopatterns coated with DXTA than those coated with nonoxidized DXT shows that DXTA remains on the surface of the PGSA nanopattern. We used the modified Anthrone method (16) of carbohydrate quantification and determined that ≈40 μg of DXTA is immobilized per cm^2 area of gecko-patterned PGSA (see SI Fig. 6), after coating the nanopatterned substrate with 5% (wt/wt) aqueous solution of DXTA and then rinsing with water.

Through the use of amine-functionalized glass with a uniform surface density of at least 2×10^{13} amine groups per mm^2, angle-resolved x-ray photoelectron spectroscopy (XPS) was used to verify the formation of imine bonds between surface bound amine groups and the aldehyde groups on the surface of DXTA-coated PGSA nanopatterns. The presence of the imine bond can be inferred from the DXTA that remains immobilized after rinsing the surface of DXTA-coated amine glass. We used the slight shift that occurs in the C(1s) peak at the C–O and C=O as an indirect indication for presence of DXTA, in accordance to previous reports (14). As illustrated in Fig. 2*c*, residual DXTA remains after washing the amine glass, whereas nonoxidized DXT (data not shown) is completely removed indicating the effective use of immobilized aldehyde groups to bond biomaterials to tissue.

Adhesive Characterization of DXTA-Modified Gecko Patterns and Optimization of Wet Tissue Adhesion. To determine the relative contribution of morphology and chemistry to tissue adhesion, shear adhesion tests on porcine intestinal tissue were performed by using PGSA polymer compositions with various elastic properties. Three different compositions of PGSA were tested, as defined by the prepolymer degree of acrylation (DA) (11) including DA = 0.3, DA = 0.3 + 5% PEG, and DA = 0.8, which have elastic moduli of 0.38, 0.80, and 10.68 MPa, respectively, as reported (11). The PGSA DA = 0.8 is more hydrophobic and has slower degradation kinetics *in vivo* (J. Bruggeman, C. Nijst, J.M.K., C. Bettinger, M. Moore,

R.L., and D. Kohane, unpublished work). We have shown a PGSA DA = 0.3 composition with 5% PEGDA to have slower *in vivo* degradation kinetics to PGSA DA = 0.3 and to be more hydrophilic, with a higher elastic modulus (J. Bruggeman, C. Nijst, J.M.K., C. Bettinger, M. Moore, R.L., and D. Kohane, unpublished work). At DA = 0.8, tissue adhesion tests (Fig. 3*a*) demonstrated a modest increase in adhesion at various DXTA concentrations compared with the nonpatterned native polymer (separation force = 1.3×10^4 N/m^2). The effect of the nanopattern on increasing adhesion force can be observed at the 0% DXTA concentration values (maximum of ≈2-fold). At the highest DXTA coating concentration of 5% (wt/vol), a decrease in adhesion was observed. PGSA DA = 0.8 have fewer hydroxyl groups available (due to high incorporation of sebacic acid) and therefore fewer anchorage points for the immobilization of DXTA, which might explain the low effect of DXTA in PGSA DA = 0.8. Interestingly, significant cumulative enhancement of morphology and chemistry was observed only at the 0.05% DXTA concentration for PGSA DA = 0.3 with 5% PEGDA, as shown in Fig. 3*c*. The increased adhesion may also have resulted from mechanical interlocking due to polymer swelling from the PEG component. Our previous work has shown a 50% increase in swelling ratio with the addition of 5% PEG to PGSA DA = 0.3 (i.e., from 10% to 15%) (11). In the compositions of PGSA DA = 0.3 (Fig. 3*b*) and PGSA DA = 0.3 with 5% PEGDA, the highest adhesion force was observed by using the 0.05% DXTA solution; quantitatively, a maximum enhancement of ≈2-fold relative to nonpatterned surfaces without the DXTA coating is observed for the both PGSA 0.3 (4.8×10^4 N/m^2 for the patterned vs. 2.5×10^4 N/m^2 for nonpatterned non-DXTA coated) and PGSA 0.3 PEG (3.5×10^4 N/m^2 for the patterned vs. 1.8×10^4 N/m^2 for nonpatterned non-DXTA coated). To determine whether rinsing of the surface affects adhesion through removal of excess DXTA, the coated surface of PGSA DA = 0.3 with 5% PEGDA gecko pattern was vigorously rinsed with deionized water, and tissue adhesion tests were performed. As shown in Fig. 3*d*, rinsing excess DXTA from the surface consistently improved adhesion. The optimal coating was determined to be 0.025% solution of DXTA followed by removal of excess DXTA through vigorous rinsing with deionized water, which led to a 4-fold enhancement in adhesion over native DA = 0.8 surfaces. SEM images of DXTA-coated PGSA nanopatterns revealed that at low DXTA concentrations of 0.05%, pillar tip interactions (tips stick together) occur in ≈50% of the pillars (Fig. 3 *e–g*), whereas at the high DXTA concentration of 5%, the nanopillars are covered by a thick layer of DXTA coating (Fig. 3*h*), which prevents the underlying patterns from contacting the tissue. This observation is a possible explanation for the decrease in adhesion observed for the 5% DXTA-coated patterns. A table in Fig. 3 shows the baseline and maximum adhesion strength achieved for each material tested.

Degradation Characteristics of Biodegradable Gecko Patterns. To understand how the gecko pattern changes as a function of biodegradation, we investigated changes in pillar geometry. PGSA patterns were degraded in a 1-M solution of sodium hydroxide, and time-lapsed optical profilometry was used to measure changes in pillar dimensions. As shown in Fig. 4*a*, pillar height decreased during degradation, whereas there was only a slight decrease in the base diameter. A decrease in pillar height resulted in an increase in pillar tip diameter, because pillars are cone shaped. These results not only suggested that the pattern remained on the surface of the PGSA polymer but also provide possible strategies to design surface patterns with tailored degradation profiles where the geometry of the pillar surfaces can be designed for the purpose of influencing the surface degradation characteristics. To investigate pattern degradation in more physiologically relevant conditions, we subjected the PGSA DA = 0.3 patterns to degradation in 1 unit/ml of cholesterol esterase (11, 17). Cholesterol esterase enzyme has been shown to be identical to the esterases associated with macrophages
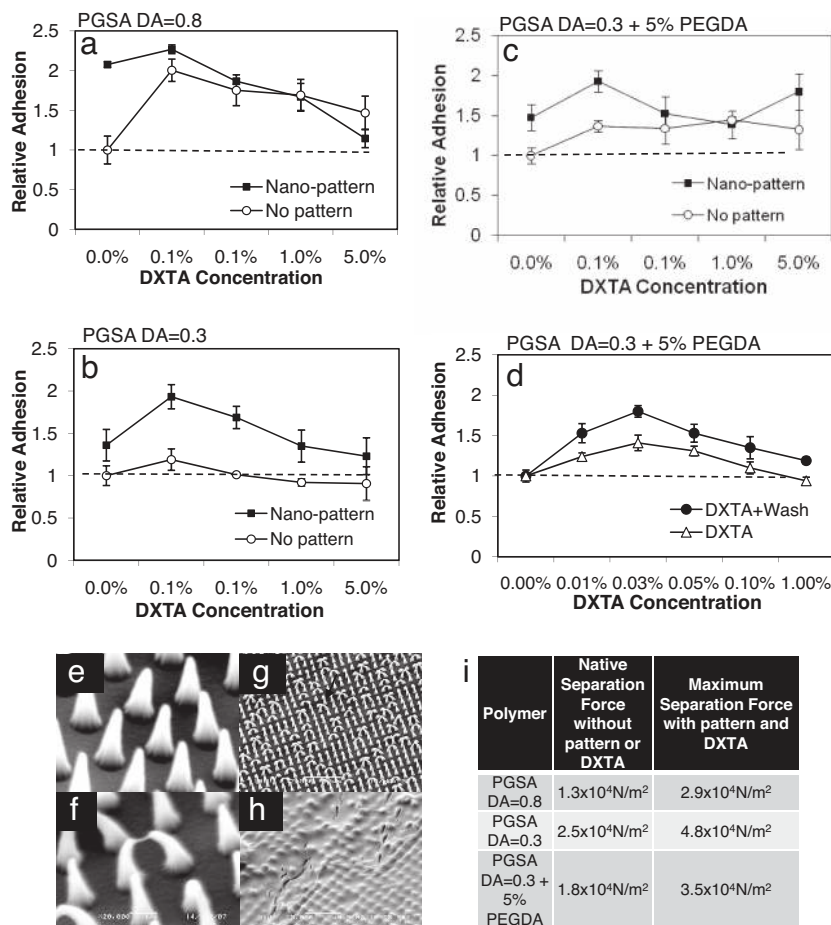
Fig. 3. DXTA coating of nanopatterned PGSA polymer improves tissue adhesion *in vitro*. (*a–c*) Relative adhesion of nanopatterned vs. unpatterned PGSA polymer to porcine tissue slides as a function of DXTA surface coating concentration. *A* represents PGSA DA = 0.8, *B* is PGSA DA = 0.3 with 5% PEGDA, and *C* is PGSA DA = 0.3. Data were normalized to the unpatterned DA = 0.8 PGSA polymer without DXTA coating. (*d*) Normalized adhesion results of the PGSA DA = 0.3 with 5% PEG DA shows the effect of washing on improving adhesion at various DXTA concentrations. (*e*) Nanopatterned PGSA polymer after surface spin coating with water as control. (*F* and *G*) Nanopatterned PGSA after surface spin coating with 0.05% DXTA solution shows adhesion of neighboring pillar tips. The black arrow indicates how DXTA polymer may cause neighboring pillar tips to stick together. (*h*) Five percent DXTA completely obstructed the underlying nanopattern. (*i*) The baseline adhesion and maximum values obtained for each material used.

that are known to degrade polyesters (17). After 8 days of degradation, SEM images of the patterns as shown in Fig. 4*b* revealed that pillars and bulk underlying the PGSA material have started to degrade. In contrast, no observable degradation of pillars occurred during the 8-day experiment in the PGSA DA = 0.8 and PGSA DA = 0.3 with 5% PGDA formulations (data not shown).

Biocompatibility of Gecko Tissue Tape. With the purpose of evaluating the effect of nanopatterned surfaces and the DXTA coating on tissue biocompatibility and adhesiveness, we implanted 1-cm^2 adhesive patches in the subfascial environment overlying the rectus muscle of rats, selected for its clinical relevance. As shown in Fig. 4*c*, flexible adhesive gecko tapes were cut into square patches and inserted into fascial flaps on the underlying rectus muscle with the nanopattern oriented outward toward the fascia. Weight-loss measurements of gecko patterns after 1-week implantation showed a negligible difference between the 0.3 and 0.3 + PEGDA PGSA patterns (Fig. 4*d*). In accordance with our previous findings (11), the PGSA with higher DA (0.8) had a smaller weight loss, which is indicative of slower degradation

Adhesive strength was determined by using a test apparatus shown in Fig. 4*e*, where explanted tissue containing the adherent patch was fixed on a glass slide, and a defined mechanical shear force was applied. As the results in Fig. 1 *c* and *d* suggest, a decrease in the tip diameter to pitch ratio (T/P) actually leads to an enhancement in adhesion. In other words, maximum enhancement occurs for the pattern with the lowest density of pillars. This observation is counterintuitive, because previous work on patterned adhesion demonstrated that enhancement is based on the mechanism of contact line splitting that requires maximizing the pillar density (18). However, our materials are unique in that the

pillars are interfacing with another soft compliant surface, i.e., the deformable tissue. Although additional experimental results are necessary for confirmation, one possible means of enhancement is associated with the enhanced conformal contact between the tissue and PGSA patterned adhesive. As Fig. 4*d* illustrates, within a narrow range the tissue can better conform to the patterned adhesive surface when the distance between pillars is sufficiently large and the tip diameter sufficiently low (Fig. 4*f*). Otherwise, the tissue cannot conform to the area between the pillars and reduces the interfacial contact area (Fig. 4*f*). Hence, for a constant pillar height, the ratio T/P is an empirical descriptor that describes the ability for the tissue interface to conform to the patterned surface and increase the interfacial contact area.

To determine whether improved adhesion from DXTA coating is maintained over time, adhesion of the gecko patterns was measured after 48 h of implantation. As shown in Fig. 4*g*, the adhesive strength of DXTA-coated gecko patterns was >2-fold higher than samples without the DXTA coating.

To assess the effect of polymer composition and nanotopography on tissue response, disks of patterned PGSA polymer were implanted subcutaneously in the backs of rats for 7 days. In agreement with reported observations (12, 19), the tissue response was mild (Fig. 4 *h* and *i*) and did not depend on PGSA nanotopography or formulation (Fig. 4 *j–m*). As reported by a blinded pathologist, a thin inflammatory infiltrate layer with little vascularization encircled the implant cavity, similar to previous implantation studies. No giant cell reaction was observed. The chronic inflammation to nonresorbable polyurethane (Fig. 4*m*), which was used as a control, was more pronounced, because the cellular infiltrate surrounding the implant had distinctive papillary architecture with increased vascularity and edema. The tissue response was not assessed in the

Mahdavi *et al.*

Fig. 4. *In vivo* characterization of synthetic tissue tape. (*a*) Time-lapsed optical profilometry measurements of pillar dimensions during *in vitro* degradation in 1 M sodium hydroxide solution (color scheme as in Fig. 1*b*). (*b*) SEM image of PGSA DA = 0.3 gecko-patterned surface shows presence of pillars after eight days of *in vitro* degradation under physiological conditions in 1 units/ml of cholesterol esterase enzyme. (Scale bar, 10 μm.) (*c*) Representative image of 1-cm² patches of gecko tissue tape, which were used for *in vivo* experiments. Elasticity of the samples is demonstrated through stretching and bending of the samples using forceps (*Inset*). (*d*) Weight-loss measurements after 1 week implantation of samples with different compositions of PGSA and a polyurethane control (PU). (*e*) Shear adhesion tests were performed on explanted tissue. (*f*) Within a narrow range, patterned adhesives may exhibit enhanced surface area of contact with tissue when the distance between pillars are sufficiently large and the tip diameter sufficiently low. (*g*) *In vivo* adhesion strength of DXTA-coated PGSA DA = 0.8 samples after being implanted for 48 h. (*h* and *i*) Tissue response to nanopatterned PGSA disks with DA = 0.8, s.c. implanted in the rat dorsum. Low-magnification photomicrographs of (*h*) H&E and (*i*) Masson's trichrome-stained tissue sections immediately adjacent to PGSA implants. PGSA implants formerly occupied open spaces denoted by *. Nanotopography was placed next to muscle tissue (down), and samples were harvested after 1-week implantation. A mild response was observed with a thin inflammatory infiltrate without collagen deposition. (Scale bar, 400 μm.) (*j–m*) High-magnification photomicrographs of H&E-stained tissue sections immediately adjacent to PGSA implants with (*j*) DA = 0.3, (*k*) DA = 0.3 with 5% PEGDA, and (*l*) DA = 0.8 and (*m*) unpatterned polyurethane implants. Nanotopography was placed next to muscle tissue (down), and samples were harvested after 1-week implantation. The tissue responses were mild in all PGS implantation but more pronounced in the polyurethane implantation. (Scale bar, 100 μm.)
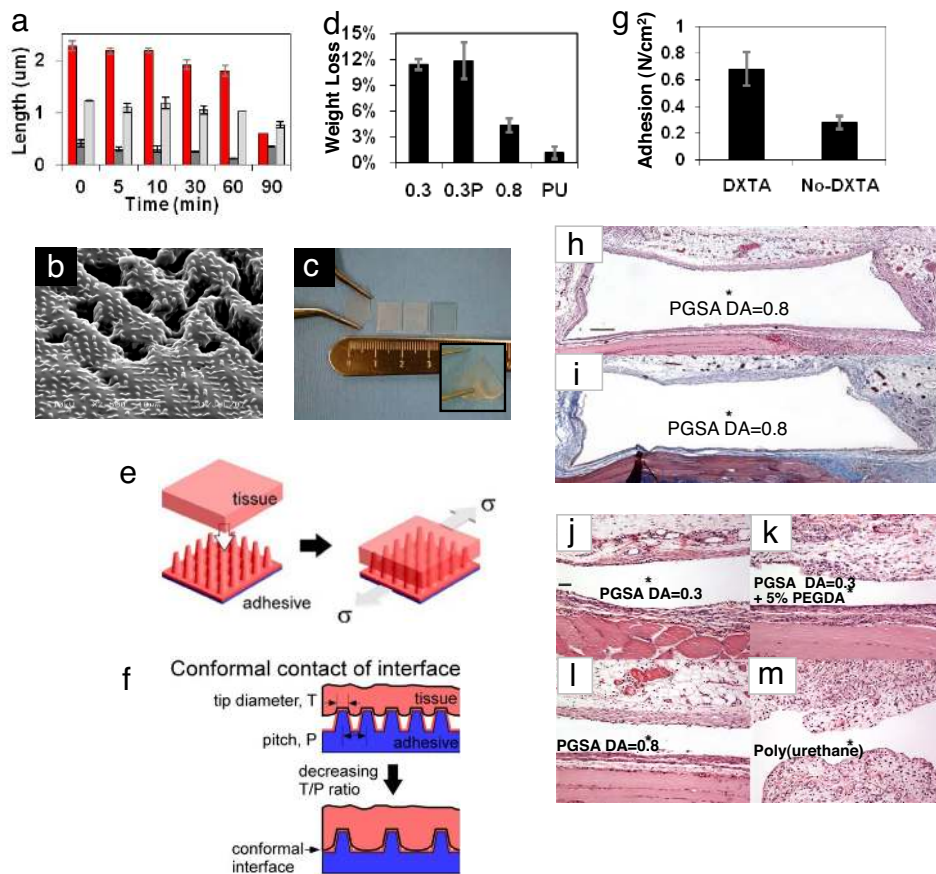
functional tests for the materials that were implanted in the preperitoneal space. This functional model provided the benefit of evaluating the adhesiveness of the material in contact with two unique tissue surfaces. Extensive surgical manipulation of the tissue was required, which induced some expected muscle degradation with marked fibroblastic proliferation that masked any inflammatory response to the implanted materials. Taken together, these results suggest that introduction of gecko nanopatterned substrates or the DXTA coating on the surface of the PGSA polymer did not result in an increased tissue response to the implant. Therefore, a general strategy of using a judicious choice of surface patterning with tissue-compatible surface chemistry can provide an effective means to achieve tissue adhesion.

The mechanism of enhancement in our materials is based on mechanical interlocking with the tissue. Compared with the gecko and other gecko-based adhesives, which are based on spatular surface contact and weak reversible adhesion, strong single-use tissue adhesives require additional mechanisms, such as mechanical interlocking and covalent chemistry. Unlike the gecko, permanent deformation of the interface may occur during debonding. Although this mechanism differs significantly from that of the gecko, i.e., contact line splitting, the basic principles of adhesion enhancement are similar: intelligent design of a patterned interface to enhance interfacial contact.

Conclusions

Through screening a variety of nanopatterned morphologies and exploring the cumulative effects of surface morphology with chemistry using a biocompatible and biodegradable elastomer, we have developed a tissue-compliant synthetic gecko-inspired adhesive that may be useful for a range of medical applications. *In vivo* characterization of implanted gecko tapes demonstrated minimal tissue response. Therefore, this strategy may provide an effective method for the development of tissue adhesives that can potentially provide a platform for many practical and useful additions to the surgical armamentarium.

Materials and Methods

Nanomolding of PGSA Polymer. Nanomolds were fabricated by using photolithography followed by reactive ion etching of an oxide layer on a silicon wafer. Oxidation of silicon wafers and incorporation and development of resist films are described in *SI Text*. The photomask was fabricated by Photronics. The wafer was then ashed in a March barrel asher for 30 seconds at 55 W in a 250-mTorr oxygen plasma. Reactive ion etching was then used to transfer the pattern of hole arrays into the oxide layer to form the mold. We used a Surface Technology Systems (STS) Multiplex Reactive ion etching with gas flows of 14.4 standard cubic centimeters per minute (sccm) of CHF_3 and 1.6 sccm of CF_4 at 20-mTorr pressure. An oxide etch rate of ≈2.8 nm/second was achieved by using 200 W of radiofrequency power. Three mold depths were targeted by controlling the etch time, with approximate depths of 1, 2, and 3.5 μm. After etching, the resist layer was removed by sequential rinse in acetone and SVC-12 (Microchem) for 30 min each and EKC-270 stripper (DuPont) for 2.5 h followed by a 10-min rinse with deionized water and spin drying. The etched oxide depth was measured by profilometry on a Tencor Alpha-Step-IQ. To develop patterned polymer surfaces, PGSA prepolymer was poured onto silicon molds without applying vacuuming and was UV-cured as described (11). The macroscopic film thicknesses for all of the polymer adhesives were kept constant at 0.94 ± 0.03 mm.

Shear Adhesion Tests. Shear adhesion tests were performed on the polymer surfaces using an Electroforce ELF 3200 mechanical tester (Bose-Enduratec) con-

trolled by WinTest software (Ver. 2.51) using custom-fabricated stainless steel tissue grips and a 250-g load cell (model 31-1435-03; Sensotech). This test of shear resistance provided a measure of the ability of the patterns to resist lateral movements on tissue once immobilized. To test adhesion, 4-mm discs of the polymer were cut out of patterns using a dermal biopsy punch (Miltex Instrument) and glued to a glass slide to provide a flat adhesive surface with well defined area. Porcine intestine tissue was cut into 2×2-cm sections and glued to a glass slide using cyanoacrylate glue, and the outer surface of the intestine tissue was used for adhesion tests. The sample and tissue slides were positioned parallel to each other to provide contact between the tissue and patterned polymer sample. The position of the test samples was identical for all samples to minimize sample-to-sample variance in the initial contact or preload force. Upon initiation of the adhesion test, the tissue slide was displaced at a rate of 8 mm/min while the force was recorded.

Synthesis and Characterization of DXTA. DXTA was synthesized as described (20) (*SI Text*). The DXTA solution was spin-coated on the surface of the PGSA gecko pattern using a speed of 4,000 rpm, which was determined to be optimal for a uniform surface coating. DXTA hydrogels have an elastic modulus between 20 and 60 kPa, depending on the degree of cross-linking as described (21).

XPS and FTIR Analysis. XPS and FTIR measurements were carried out on an Axis Ultra spectrometer (Kratos Analytical) and a Nicolet Magna 860 FTIR instrument, respectively. Please see *SI Text* for the operating conditions.

***In Vivo* Characterization of Implanted Gecko Tissue Tape.** *Surgical procedures.* All surgical procedures were approved by the Institutional Animal Care and Use Committee of the Massachusetts General Hospital and performed according to the National Institutes of Health Guidelines for the Care and Use of Laboratory Animals. See *SI Text* for details.
Biocompatibility studies. The tissue response was determined for nanopatterned PGSA materials (DA = 0.3, DA = 0.3 with 5% PEGDA, and DA = 0.8) and the control material, unpatterned nonresorbable polyurethane. For each PGSA formulation, 5-mm-diameter disks were punched from polymer sheets of 1.1-mm thickness using dermal biopsy punches (Acuderm, Acu-Punch) and dried at 60°C at 50 torr for 48 h and disinfected by UV light. Disks were s.c. implanted into pockets on the backs of five Wistar rats ($n = 8$ for each PGSA formulation; $n = 6$ for polyurethane). A small incision was made in the dorsal midline of each animal. Six small s.c. pockets deep inside the loose areolar tissue were developed using blunt dissection bilaterally over the scapular and the *latissimus dorsi* regions and

caudal to the pelvic brim. One sterile PGSA disk was inserted into each pocket, with the nanopattern facing the muscle, and each incision was closed with 2–0 silk sutures. One week after implantation, the rats were killed and samples located by palpation. Each PGS disk was excised with all associated surrounding dermal and muscle tissues.
Functional adhesion studies. Tissue adhesion of DXT-coated nanotextured 0.8 acrylation PGS samples was evaluated in the subfascial environment. A small incision was made in the ventral midline of each animal ($n = 7$). Dissection was carried down to the linea alba, and all loose areolar tissue was gently swept off the abdominal wall using damp gauze. After identifying the fascia, a small incision parallel to the linea alba was made bilaterally in the ventral aspect of the rectus sheath. A small fascial flap was developed using a blunt dissection technique on each side of the incision. A sample (1×1 cm, 1.1-mm thick) was placed in each flap on the exposed underlying rectus muscle with the nanopattern oriented outward toward the fascia; one nanopatterned/DXT-coated sample and one nanopatterned/uncoated sample were inserted into each animal. The overlying tissues were reapproximated, and the skin was closed with 2–0 silk sutures. Rats were killed after 48 h for adhesive testing. After shaving, the entire abdominal wall was removed, and the samples were identified by palpation. Each explant was excised from the abdominal wall with associated surrounding tissues from the dermis to the underlying muscle layer. Samples for adhesion testing were immersed in sterile saline and tested immediately after removal. The samples explanted at 7 d ($n = 3$) were prepared for histologic analysis.
PGSA explantation. For weight loss, the PGSA explants were carefully dissected from the surrounding tissue and rinsed in distilled water, dried at 60°C for 48 h at 50 torr vacuum, and weighed. For histological evaluation, the tissue surrounding the implant was carefully trimmed ($2 \times 2 \times 0.5$ cm), and both the tissue and sample were fixed in 10% buffered formalin. After 3 days, the tissue samples were cut in half, the capsules were incised, and the polymer disks were removed. Tissue was cut into 3-mm-wide sections and embedded in paraffin. Sections (6-μm thick) were stained with H&E and Masson's trichrome and analyzed for the degree of inflammation and fibrosis. The tissue response was characterized based on the level of neutrophils, lymphocytes, macrophages, and giant cells. Fibrosis was identified primarily by collagen deposition.

1. Autumn K, Liang YA, Hsieh ST, Zesch W, Chan WP, *et al.* (2000) Adhesive force of a single gecko foot-hair. *Nature* 405:681–685.
2. Pennisi E (2000) Biomechanics. Geckos climb by the hairs of their toes. *Science* 288:1717–1718.
3. Autumn K, Sitti M, Liang YA, Peattie AM, Hansen WR, *et al.* (2002) Evidence for van der Waals adhesion in gecko setae. *Proc Natl Acad Sci USA* 99:12252–12256.
4. Hansen WR, Autumn K (2005) Evidence for self-cleaning in gecko setae. *Proc Natl Acad Sci USA* 102:385–389.
5. Sun W, Neuzil P, Kustandi TS, Oh S, Samper VD (2005) The nature of the gecko lizard adhesive force. *Biophys J* 89:L14–17.
6. Huber G, Mantz H, Spolenak R, Mecke K, Jacobs K, *et al.* (2005) Evidence for capillary contributions to gecko adhesion from single spatula nanomechanical measurements. *Proc Natl Acad Sci USA* 102:16293–16296.
7. Autumn K, Hansen W (2006) Ultrahydrophobicity indicates a non-adhesive default state in gecko setae. *J Comp Physiol* 192:1205–1212.
8. Geim AK, Dubonos SV, Grigorieva IV, Novoselov KS, Zhukov AA, Shapoval SY (2003) Microfabricated adhesive mimicking gecko foot-hair. *Nat Mater* 2:461–463.
9. Crosby AJ, Hageman M, Duncan A (2005) Controlling polymer adhesion with ''pancakes''. *Langmuir* 21:11738–11743.
10. Lee H, Lee BP, Messersmith PB (2007) A reversible wet/dry adhesive inspired by mussels and geckos. *Nature* 448:338–341.
11. Nijst CL, Bruggeman JP, Karp JM, Ferreira L, Zumbuehl A, *et al.* (2007) Synthesis and characterization of photocurable elastomers from poly(glycerol-cosebacate). *Biomacromolecules* 8:3067–3073.
12. Wang Y, Ameer GA, Sheppard BJ, Langer R (2002) A tough biodegradable elastomer. *Nat Biotechnol* 20:602–606.
13. Autumn K, Dittmore A, Santos D, Spenko M, Cutkosky M (2006) Frictional adhesion: a new angle on gecko attachment. *J Exp Biol* 209:3569–3579.
14. Wang DA, Varghese S, Sharma B, Strehin I, Fermanian S, Fairbrother DH, Cascio B, Elisseeff JH (2007) Multifunctional chondroitin sulphate for cartilage tissue-biomaterial integration. *Nat Mater* 6:385–392.
15. Mo X, Iwata H, Matsuda S, Ikada Y (2000) Soft tissue adhesive composed of modified gelatin and polysaccharides. *J Biomater Sci Polym Ed* 11:341–351.
16. Somani BL, Khanade J, Sinha R (1987) A modified anthrone-sulfuric acid method for the determination of fructose in the presence of certain proteins. *Anal Biochem* 167:327–330.
17. Santerre JP, Labow RS (1997) The effect of hard segment size on the hydrolytic stability of polyether-urea-urethanes when exposed to cholesterol esterase. *J Biomed Mat Res* 36:223–232.
18. Chan E, Greiner C, Arzt E, Crosby A (2007) Design model systems for enhanced adhesion. *MRS Bull* 32:496–503.
19. Sundback CA, Shyu JY, Wang Y, Faquin WC, Langer RS, Vacanti JP, Hadlock TA (2005) Biocompatibility analysis of poly(glycerol sebacate) as a nerve guide material. *Biomaterials* 26:5454–5464.
20. Maia J, Ferreira L, Carvalho R, Ramos MA, Gil MH (2005) Synthesis and characterization of new dextran-based hydrogels. *Polymer* 46:9604–9614.
21. Ferreira L, Gil MH, Dordick JS (2002) Enzymatic synthesis of dextran-containing hydrogels. *Biomaterials* 23:3957–3967.